RSC Advances

PAPER

View Article Online
View Journal | View Issue

Cite this: *RSC Adv.*, 2024, **14**, 32451

Constructing covalent organic frameworks with dense thiophene S sites for effective iodine capture†

Yiling Ran,[abc] Yi Wang,[c] Man Yang,[c] Jian Li,[c] Yan Zhang *[a] and Zhanguo Li *[c]

Developing versatile sorption materials for radionuclides (*e.g.* iodine) capture has been a critical goal in nuclear energy and environmental science. At the same time, covalent organic frameworks (COFs), on account of their high porosity and functional scaffolds, have opened up a new way to develop adsorbents in recent years. Herein, two kinds of COF materials containing thiophene (TAPT-COF and TAB-COF), as iodine sorbents, are designed and synthesized by Schiff base reaction. Among them, TAB-COF has a higher surface area (TAPT-COF: 1141 $m^2 g^{-1}$, TAB-COF: 1378 $m^2 g^{-1}$), which is helpful for the physical iodine adsorption. More importantly, the COF backbone is rich in both N and S sites, which is advantageous to the chemical adsorption of iodine. These two features make the two COFs ideal iodine sorption materials. For example, TAB-COF has an excellent gaseous iodine adsorption capacity (2.81 g g^{-1}) and is one of the most efficient iodine adsorption materials. Meanwhile, TAB-COF has an excellent adsorption effect on iodine in the cyclohexane system, which can reach 200 mg g^{-1}. In addition, the DFT calculations proved that both imine N and thiophene S serve as active sites during the iodine adsorption. TAB-COF exposes more active sites on the premise of having a higher surface area, thereby leading to a higher iodine adsorption capacity. The results here indicate improved sorption efficacy by introducing thiophene in COFs for sorption applications in general and especially pave the way for developing stable and effective COF sorbents for iodine capture from various environments.

Received 2nd September 2024
Accepted 7th October 2024

DOI: 10.1039/d4ra06333c

rsc.li/rsc-advances

Introduction

In order to solve the global energy crisis, many countries have turned to nuclear power stations as the first choice to provide a large amount of clean energy. In addition, the excessive use of fossil fuels by power stations leads to the release of large amounts of carbon dioxide, sulfur oxides, and particulate matter into the atmosphere, causing environmental problems such as global warming.[1] Nuclear energy is a technology that can provide a stable supply of electricity without producing CO_2. Therefore, nuclear power generation plays a significant role in the use of clean energy. Nuclear power stations generate more than 11% of the world's electricity.[2] However, the issues of safe handling of spent fuel and waste disposal need to be solved.[3,4] Nuclear power plants are related to several radioactive and volatile substances during operation, including ^{14}C, ^{85}Kr, ^{129}I, and ^{3}H.[5] Radionuclides are unstable substances that spontaneously break down and release radiation, and these radionuclides are easily dispersed through the atmosphere or aqueous solutions. As a result, nuclear waste containing radionuclides has safety risks and is difficult to dispose of, and will cause great harm to human beings and the environment.[6] Iodine nuclides, particularly ^{129}I, are of major concern among these radionuclides in terms of immobilization of nuclear waste. Radioactive isotopes of iodine may enter the metabolic system and accumulate in the thyroid gland, leading to human poisoning and thyroid cancer.[7,8] The separation and storage of radioactive iodine are vital for sustainable development and environmental protection.

In traditional technology, silver-doped materials are generally used as iodine adsorbents. However, this method is expensive and irreversible.[9,10] At present, solid materials with open structures, such as zeolites,[11] hydrogen-bonded organic frameworks (HOFs),[12] and porous organic polymers (POPs)[13,14] can be used for iodine adsorption due to their high porosity and good reusability. At an early stage, ion-exchange zeolites are utilized for iodine adsorption,[15] but they lack significant reusability. The effects of activated carbon and porous organic polymers (POPs) are also not obvious.[5,16,17] Some of these materials have high porosity, but there are also some disadvantages, like single-use conditions, instability in a humidity

[a]School of Chemistry, Southwest Jiaotong University, Chengdu, Sichuan 610031, China. E-mail: zyzw@swjtu.edu.cn
[b]School of Life Science and Engineering, Southwest Jiaotong University, Chengdu, Sichuan 610031, China
[c]State Key Laboratory of NBC Protection for Civilian, 102205 Beijing, China. E-mail: lizhanguo@sklnbcpc.cn

† Electronic supplementary information (ESI) available. See DOI: https://doi.org/10.1039/d4ra06333c

environment, and low adsorption capacity.[18] POPs have strong physical and chemical stability and high adsorption capacity. However, their reusability is low due to the disordered nature of their pores.[17] Therefore, it has an important meaning to search for a novel crystal adsorption material with a well-ordered structure and high adsorption capacity for iodine capture.

Covalent organic frameworks (COFs) are a new sort of crystal material. COFs have been effectively applied in adsorption because of their permanent pores, periodic structure, abundant building units, and adjustable pore structure. COFs have a high affinity to iodine on account of their excellent stability, large specific surface area, high porosity, and π–π conjugation.[19] Therefore, it has an important meaning to design COFs with high porosity and characteristic adsorption sites to improve the adsorption of iodine. Recent studies have shown that in COFs, the presence of electron-rich (N and S) can improve the adsorption of the material and the guest molecules can be adsorbed quickly. The intense interaction between the iodine molecules and the optimized dense binding sites of the porous materials is conducive to the high absorption of iodine due to the formation of charge transfer complexes.[20–23] However, the use of S-rich COFs for iodine removal is rarely studied.

Herein, two S-containing COF materials, TAPT-COF and TAB-COF, were synthesized by the solvothermal method. The adsorption capacity of TAB-COF is 2.81 g g^{-1}, which is equivalent to or greater than most porous materials that has already been reported, and it is a good iodine adsorption material. Moreover, TAB-COF has a specific adsorption for iodine in cyclohexane solution. We explored the effects of porosity, N content, and S content on the iodine adsorption performance, and we concluded that TAB-COF exposed more active sites (S sites and N sites) on the premise of a larger specific surface area, thus improving the iodine adsorption capacity of the material. Among them, the effect of sulfur content on the adsorptive iodine capacity of the material is greater than that of nitrogen content.

Results and discussion

Characterization

Based on the above, the experimental scheme was improved in combination with the relevant literature.[24] The adsorption properties of two thiophene-containing COFs for iodine were tested. TAPT-COF and TAB-COF were synthesized from benzo [1,2-*b*:3,4-*b*′:5,6-*b*″]trithiophene-2,5,8-tricarbaldehyde (BTT), 3,5-tris-(4-aminophenyl) triazine (TAPT) or 1,3,5-tris(4-aminophenyl) benzene (TAB) under a solvothermal condition (Scheme 1).[25,26] Compared with the literature, we extended the synthesis time of TAPT-COF and TAB-COF from 3d to 4d, and the crystallinity is significantly improved (Fig. 1b and S1†). Fourier infrared (FT-IR) spectra of BTT aldehyde monomer, amino monomer, TAPT-COF, and TAB-COF (Fig. 1a) show that the stretching vibrations of the –NH_2 double peaks (~3370 and 3300 cm^{-1}) in the amino ligand almost disappear in TAPT-COF and TAB-COF.[27,28] Compared with the BTT aldehyde monomer HC═O peak (~1660 cm^{-1}), the corresponding peak intensity of TAPT-COF and TAB-COF decreased significantly, indicating that most of the –CHO reaction has occurred. In addition, there is

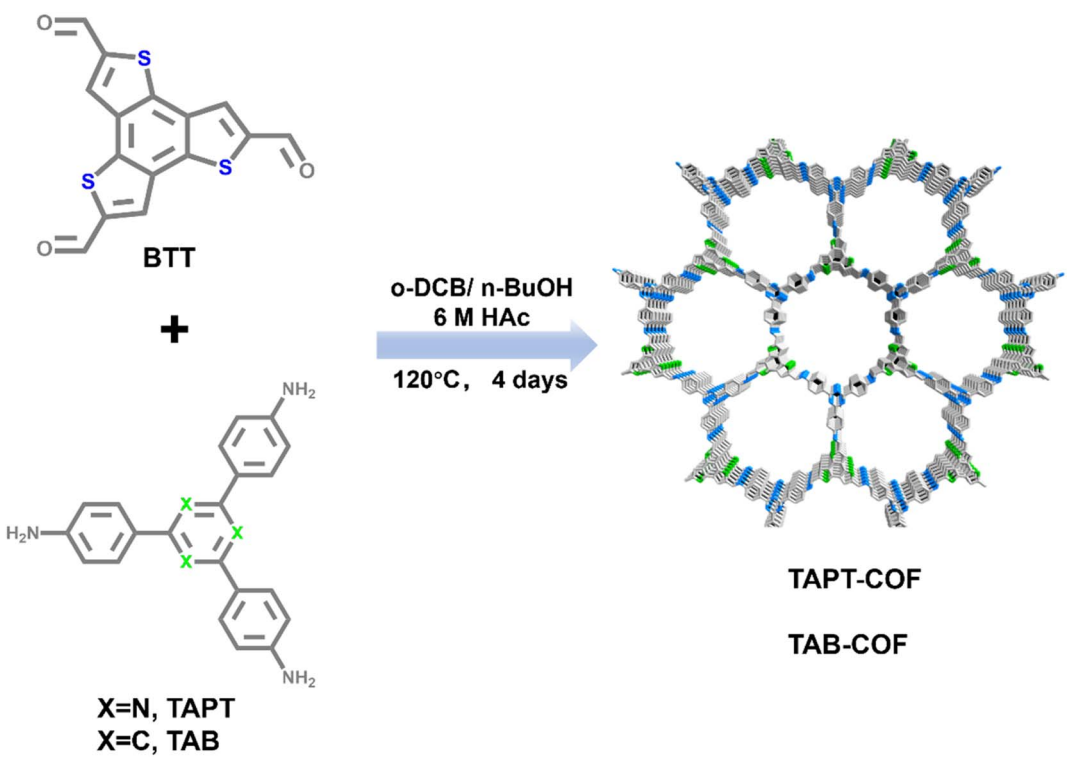

Scheme 1 Schematic synthesis of TAPT-COF and TAB-COF.

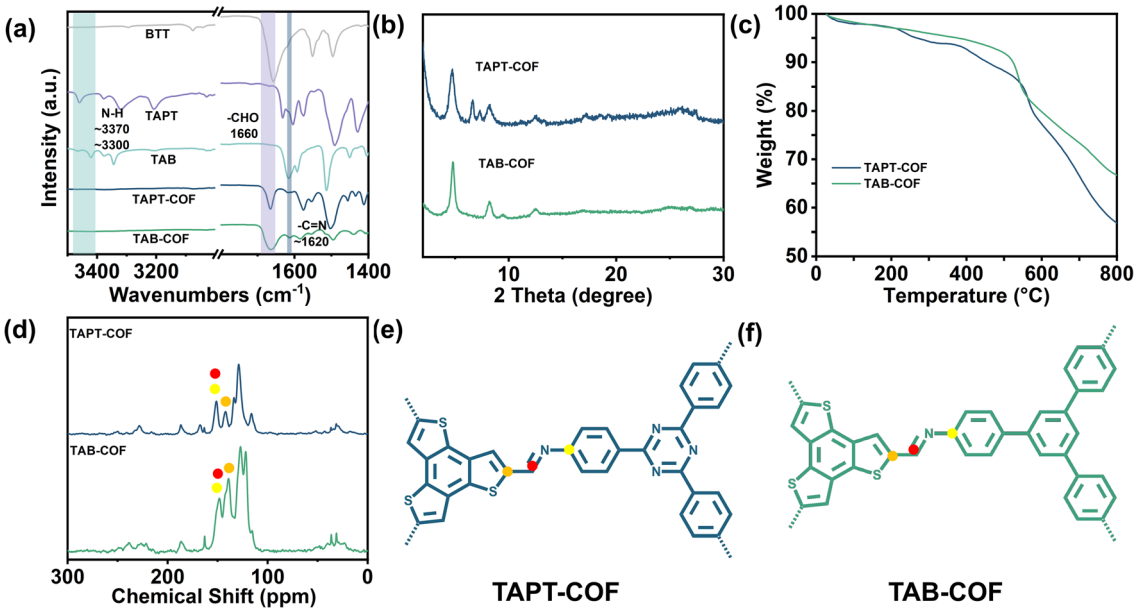

Fig. 1 (a) FT-IR spectra of the monocases, TAPT-COF and TAB-COF. (b) XRD patterns of TAPT-COF and TAB-COF. (c) TGA analysis of TAPT-COF and TAB-COF. (d) ^{13}C NMR spectra of TAPT-COF and TAB-COF. The structure of (e) TAPT-COF and (f) TAB-COF.

a characteristic peak in the two COFs spectra near 1620 cm^{-1}, which pertains to the characteristic peak of the –C═N– bond, indicating that the amino group and the aldehyde group have successfully reacted to form an imine bond.[25] The XRD pattern of the synthesized COFs shows high crystallinity (Fig. 1b), with the densest diffraction peaks appearing at about 4.7°, and the

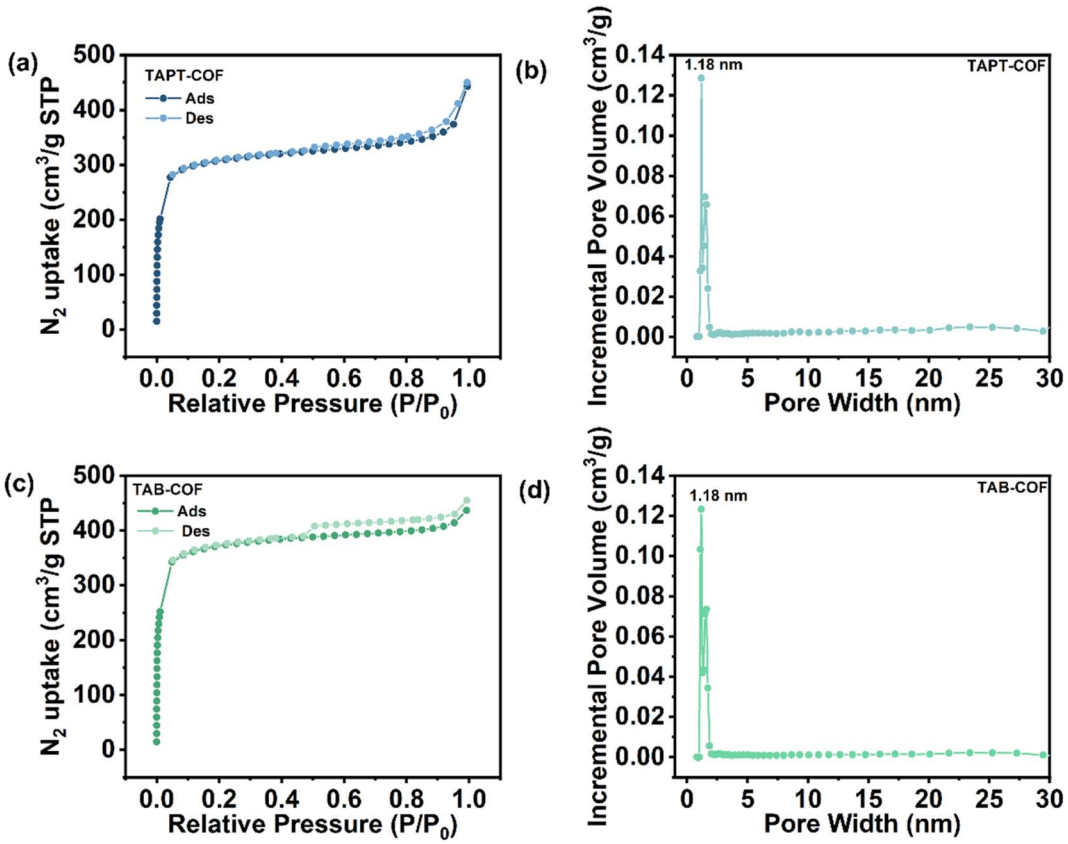

Fig. 2 N_2 adsorption/desorption isotherms of (a) TAPT-COF and (c) TAB-COF, and pore size distribution plots of (b) TAPT-COF and (d) TAB-COF.

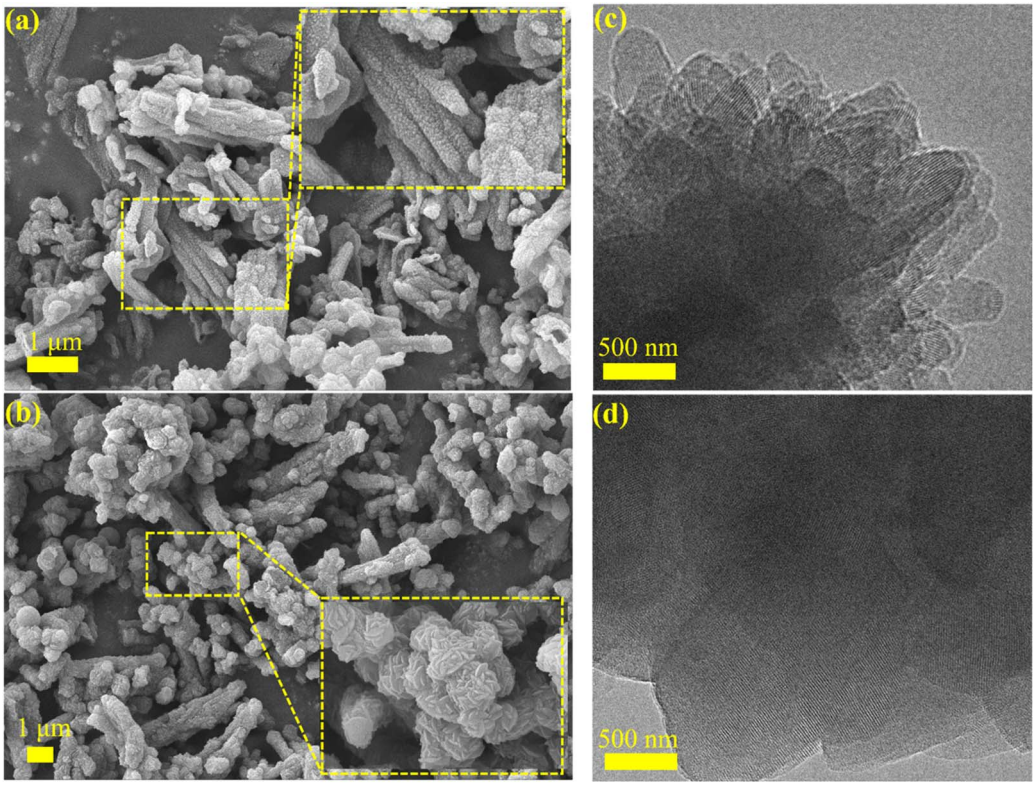

Fig. 3 SEM images of (a) TAPT-COF and (b) TAB-COF. TEM images of (c) TAPT-COF and (d) TAB-COF.

positions of each peak are in keeping with those reported in the literature.[24] In addition, ^{13}C NMR spectra shows the synthesis of TAPT-COF and TAB-COF. The characteristic peak at ~151 ppm corresponds to the C atom of the imine bond and connected C atom,[29] which means that condensation between the ammonia and aldehyde component units in TAPT-COF and TAB-COF forms the –C=N– bond (Fig. 1d–f). The peak at ~140 ppm corresponds to the thiophene-S-linked C atom, confirming the presence of thiophene.

The thermogravimetric analysis (TGA) results shown in Fig. 1c shows that the weight loss of TAPT-COF and TAB-COF is less than 15% at <500 °C, which is due to the removal of solvents in the pore of the material and the volatilization of incomplete monomers.[30] With the increase in temperature, noticeable pyrolysis of the material occurred. In the range of 500–800 °C, both COFs shows obvious weight loss. At the high temperature of 800 °C, TAPT-COF and TAB-COF still have 57% and 61% of the mass remaining, which indicates that they have good thermal stability over a wide temperature range. The surface area and pore properties of TAPT-COF and TAB-COF are evaluated by nitrogen adsorption and desorption experiments at a low temperature of 77 K (Fig. 2). The synthesized COFs have a type I adsorption–desorption isotherm. The surface areas are 1141 and 1378 $m^2 g^{-1}$, respectively. Nonlocal density functional theory (NLDFT) is used to estimate the pore size distribution of TAPT-COF and TAB-COF. The results show that TAPT-COF and TAB-COF are microporous materials with pore sizes of 1.18 nm.

The morphology of the synthesized COFs is investigated. As shown by SEM in Fig. 3a and b, TAPT-COF and TAB-COF have rod-like structures ranging in length from 0.5 μm to several microns (Fig. 3a and c). TEM images prove that TAPT-COF and TAB-COF have suitable crystal structures (Fig. 3b and d), and lattice fringes can be observed in both images. Based on EDS results (Fig. S2 and S3†), the contents of N and S in TAPT-COF are 8.79% and 10.85%, respectively. Compared with TAPT-COF, TAB-COF have higher N content (8.92%) and lower S content (10.54%).

Iodine capture, retention, and recycle

To explore the adsorption capacity of COF materials, we carried out adsorption experiments on iodine vapour and iodine-cyclohexane solution system. The adsorption capacity of two COFs to iodine vapor at 75 °C is studied by gravimetric method. The adsorption of I_2 vapor increased significantly in the first 10 hours (Fig. 4a). At about 24 h, the adsorption capacity of TAPT-COF and TAB-COF to I_2 vapor reached saturation. The color of the sample is darkened after iodine adsorption. After 96 h, the equilibrium absorption rates of TAPT-COF and TAB-COF are 1.95 and 2.81 g g^{-1}, respectively. This rapid capture of I_2 vapor and high absorption capacity demonstrate the feasibility of TAPT-COF and TAB-COF for iodine capture. The I_2 adsorption capacity of TAB-COF exceeds that of most reported adsorbents (Fig. 4d and Table S5†), such as 3D-PPy and Th-UiO-66-$(NH_2)_2$.[31,32] We believe that the high iodine-trapping capacity of TAB-COF may be due to the combined influence of the high

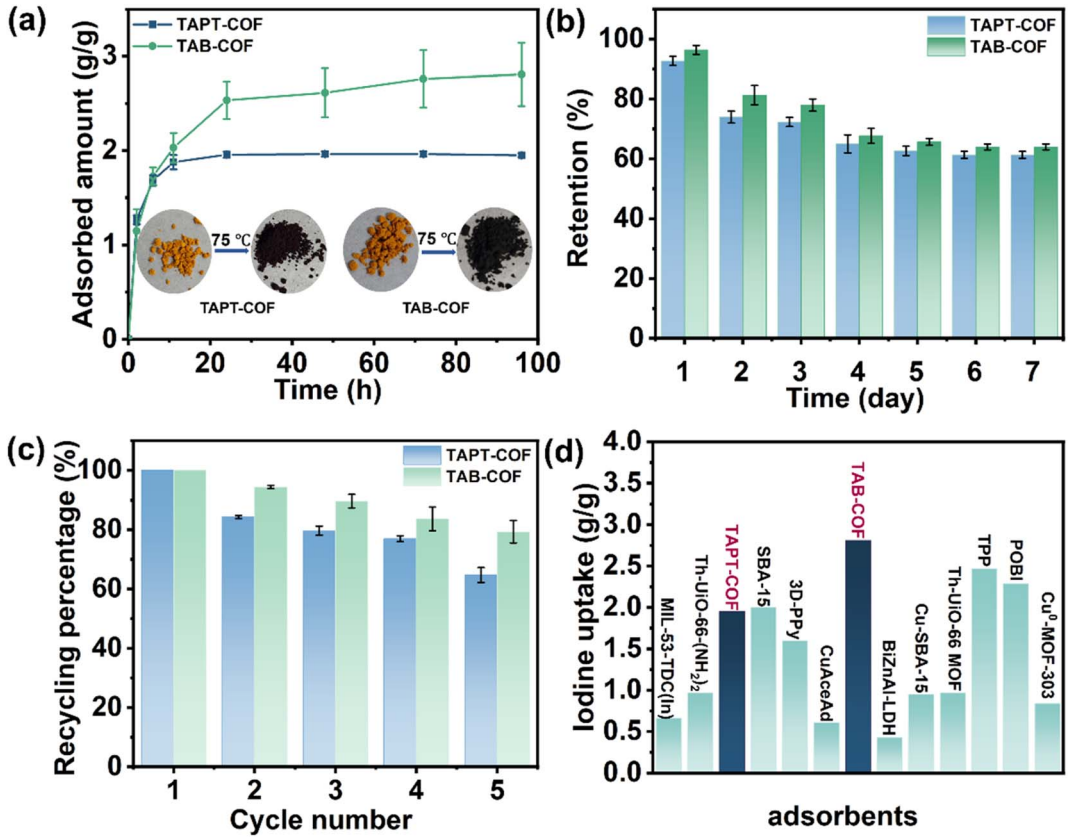

Fig. 4 (a) Change of iodine absorption with time at 75 °C. (b) Iodine retention of COFs in the atmospheric environment. (c) Recyclability of TAPT-COF and TAB-COF for the adsorption of I_2. (d) Comparison of iodine adsorption capacities in different adsorbents.

surface area of the COF materials and the binding sites (N and S).[33] As shown in Fig. S4 and S5,† the fitting of the I_2 vapor adsorbed by TAPT-COF and TAB-COF show that the adsorption process mainly conforms to the pseudo-second-order kinetic model. The $R^2 > 0.99$ indicates that the adsorption of TAPT-COF and TAB-COF on I_2 vapor is mainly chemical adsorption.[7] SEM images show that the morphology of COFs don't change after iodine adsorption, indicating good morphological stability (Fig. S6 and S7†). In addition, EDS results, as shown in Fig. S8 and S9,† which are proved the uniform distribution of iodine in the two COF materials, and confirmed the adsorption of iodine by TAPT-COF and TAB-COF.

To explore the retention rates of TAPT-COF and TAB-COF after iodine adsorption, we placed them under environmental conditions and observed their weight changes. The retention rate of TAPT-COF and TAB-COF reached 62% within 7 days and 64% within 7 days (Fig. 4b), indicating that both materials have high retention rates and can store iodine in the pores, among which TAB-COF has the highest retention rate. The reusability of materials is also a critical factor in practical applications.

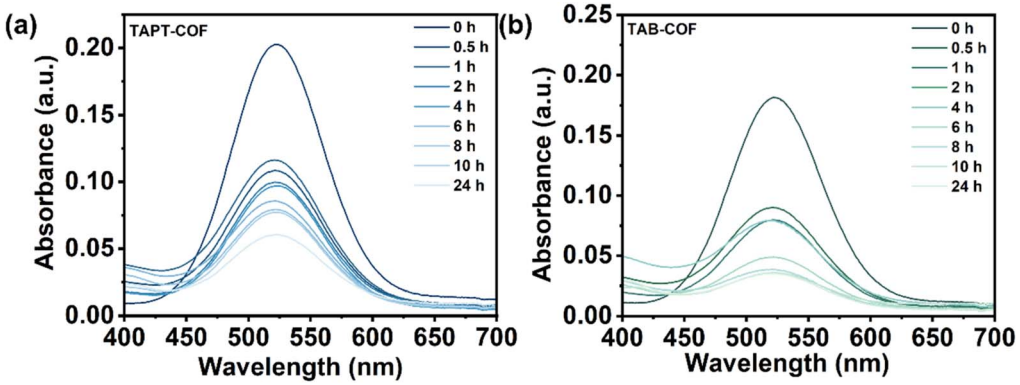

Fig. 5 UV-vis spectra of the gradual capture of iodine from cyclohexane solution for (a) TAPT-COF and (b) TAB-COF.

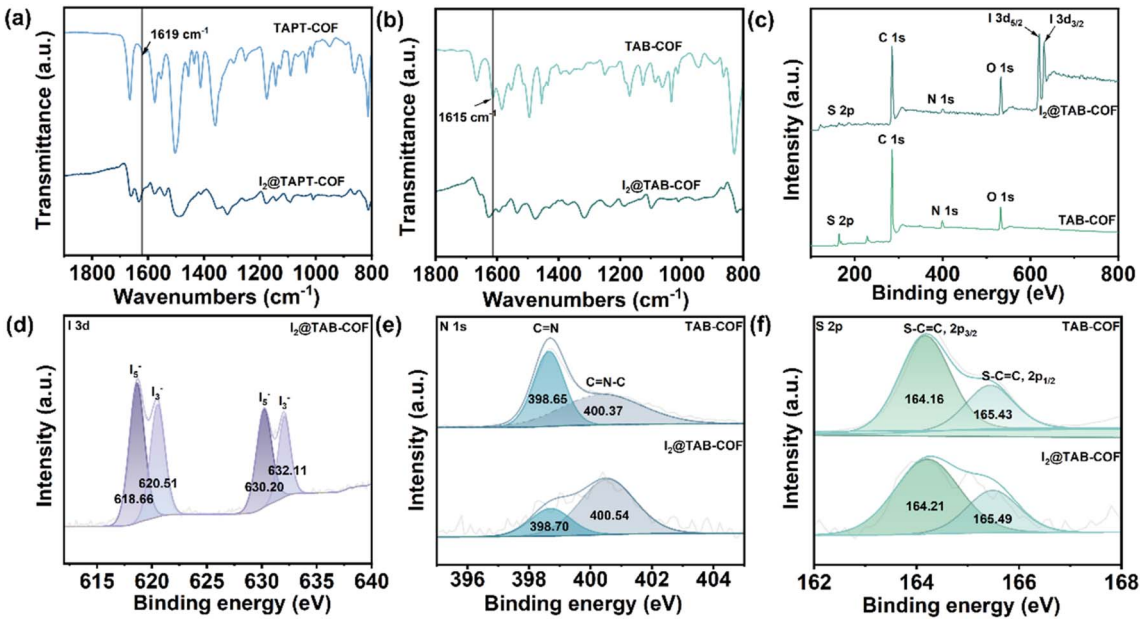

Fig. 6 FT-IR spectra of (a) TAPT-COF and (b) TAB-COF before and after iodine capture. (c) XPS spectra of TAB-COF and I_2@TAB-COF. (d) I 3d, (e) N 1s, and (f) S 2p high-resolution XPS spectra of TAB-COF and I_2@TAB-COF.

After 5 cycles, both COFs maintained good reusability, with TAPT-COF reaching 65% of first use and TAB-COF reaching 79% of first use (Fig. 4c).

Adsorption of iodine in solution

In spent fuel reprocessing, I_2 exists in a dissolved state in the solution. Considering that TAPT-COF and TAB-COF have good adsorption capacity for iodine vapor, we studied their adsorption capacity for I_2 in solution. I_2 doesn't undergo charge transfer in a cyclohexane solution.[34] Therefore, the iodine-cyclohexane solution was used to simulate the iodine-containing solution to study the adsorption effect of the prepared COF materials on the iodine in the solution. The content of iodine in the iodine/cyclohexane solution is determined by ultraviolet spectrophotometry (Fig. S10†). As shown in Fig. 5 and S11,† after the COF materials were put into cyclohexane solution, the purple color of the solution gradually faded with the increase of adsorption time (more than 24 h). The adsorption capacity of TAPT-COF is 175 mg g^{-1}, and that of TAB-COF is 200 mg g^{-1} (Fig. 5a and b), indicating that the latter has better adsorption capacity. By fitting the iodine adsorption data with the cyclohexane solution data (Fig. S12 and S13†), it was found that the iodine adsorption kinetics curves of the two COF materials in cyclohexane solution mainly conform to the pseudo-second-order kinetic model, the $R^2 > 0.99$, manifesting chemical adsorption led the interaction between COF materials and iodine.[35]

Adsorption mechanism of iodine

The mechanism of iodine adsorption by COF materials was studied by FT-IR, where I_2@TAPT-COF and I_2@TAB-COF represent TAPT-COF and TAB-COF after iodine adsorption, respectively. As shown in Fig. 6a and b, compared with the original COF FT-IR data, the C=N vibration peaks of COF materials after iodine adsorption at about 1620 cm^{-1} disappear. These changes indicate a charge shift interaction between the iodine and the C=N bond, indicating the presence of chemical adsorption.[24] In addition, the surface element composition and chemical states of TAPT-COF and TAB-COF before and after I_2 vapor adsorption are analyzed by XPS. The full spectra of TAPT-COF and TAB-COF before and after iodine adsorption are compared and analyzed (Fig. 6a and S14†), and the characteristic peak I 3d was found, indicating that iodine had been successfully adsorbed on the synthesized COF materials. The XPS spectra of I 3d, N 1s, and S 2p provide further information on the interaction mechanism. As shown in Fig. 6d and S15,† four similar characteristic peaks appear in the I 3d XPS spectra of I_2@TAB-COF and I_2@TAPT-COF, belonging to I_3^- and I_5^- respectively, indicating that adsorbed iodine exists in the form of polyiodides in COFs.[36] By comparing the relative peak intensity of I_3^- and I_5^- in the I 3d XPS spectrum, it is found that the content of I_5^- is similar to that of I_3^-, indicating that I_5^- and I_3^- are the primary forms of iodine adsorption. It is further suggested that the iodine adsorption by COFs is mainly through chemical adsorption.[37,38] Fig. 6e shows the N 1s XPS spectra of TAB-COF and I_2@TAPT-COF. In the N 1s XPS spectrum, two peaks are generated at 398.65 and 400.37 eV, the correspondences are C=N and C=N–C peaks of the imine bond, respectively, and the positions of these two peaks are shifted after the adsorption of iodine. The binding energy signature shifted significantly towards higher energies (398.70 and 400.54 eV), indicating a strong charge transfer interaction between the imine bond and iodine.[39,40] The S 2p XPS spectra at 164.16 and 165.43 eV belong to the S–C=C bond (Fig. 6f). Similarly, after iodine adsorption, the S 2p binding energy of TAB-COF also

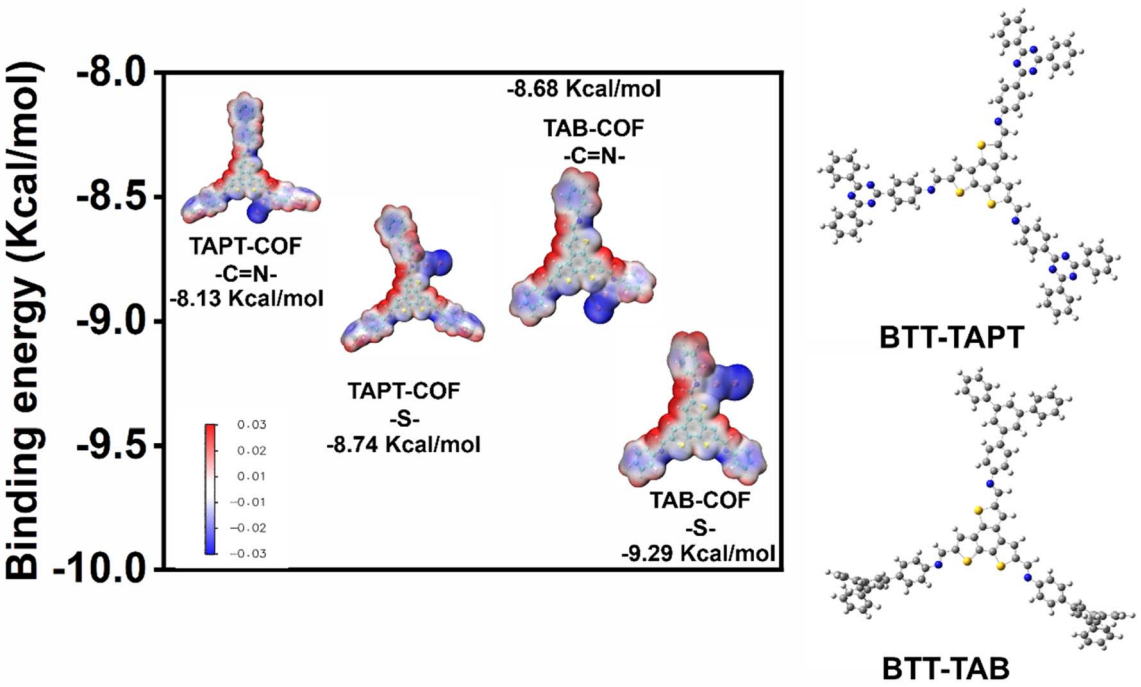

Fig. 7 Molecular van der Waals (vdW) surface images of different sites of TAPT-COF and TAB-COF with I_2. The corresponding surface local minima and maxima are shown in blue and red, respectively. BTT-TAPT and BTT-TAB structures are shown on the right-hand side.

moved significantly towards higher energy, increasing from 164.16 and 165.43 eV to 164.21 and 165.49 eV, further indicating that charge transfer occurred between S and iodine. The same is true of TAPT-COF (Fig. S16 and S17†). These results suggest that I_2 has a strong charge-transfer interaction with TAPT-COF and TAB-COF imine bonds and thiophenes.

DFT calculation

By density functional theory (DFT) calculation, the adsorption mechanism of iodine is analyzed. The internal factors leading to the difference in adsorption capacity are determined. The charge density distributions of TAPT-COF and TAB-COF containing iodine are shown in Fig. 7. To further reveal the interaction between COFs and iodine, we calculated the interaction of N and S sites with iodine in TAPT-COF and TAB-COF. As shown in Fig. 7, BTT-TAPT and BTT-TAB are model molecules representing TAPT-COF and TAB-COF, respectively. The charge density distribution of TAPT-COF and TAB-COF after I_2 adsorption are shown in Fig. 7. To further elucidate the interaction of iodine molecules with COF porous materials, we calculate the interaction of I_2 with TAPT-COF and TAB-COF. For TAPT-COF, the binding energies of iodine to N and S are -8.13 and -8.74 kcal mol^{-1}, respectively. The binding energies of TAB-COF are -8.68 and -9.29 kcal mol^{-1}, respectively. This indicates that N and S are the active sites of TAPT-COF and TAB-COF, and the two active sites have similar adsorption capacity for iodine. The results of DFT calculation are consistent with those of XPS analysis, and both proved that N and S are the iodine binding sites of TAPT-COF and TAB-COF. However, the iodine adsorption capacity of TAB-COF is greater than that of TAPT-COF because the former has a larger surface area than the latter, resulting in more S and N sites exposed in TAB-COF. This is in line with the results of iodine adsorption experiment, and the adsorption of iodine by TAB-COF is higher than that by TAPT-COF.

Conclusion

In summary, thiophene-containing COFs with two imine bonds are synthesized by the solvothermal method, and their iodine adsorption properties in the gas phase and solution are investigated. The high surface area and abundant active sites of TAPT-COF and TAB-COF make them have excellent adsorption capacity for iodine in iodine vapor and cyclohexane system. The high surface area of TAB-COF is conducive to the adsorption of iodine (2.81 g g^{-1}), which is better than most adsorbents found in the literature. The iodine adsorption capacity of TAB-COF in iodine-cyclohexane solution reached 200 mg g^{-1}. The mechanism of iodine adsorption by COF is verified by experiments and DFT calculation, and it is proved that imine N and thiophene S in TAPT-COF and TAB-COF are the adsorption sites of iodine. Compared with TAPT-COF, TAB-COF has a larger surface area and exposes more adsorption sites. Hence, the adsorption capacity of TAB-COF for gaseous iodine and iodine in solution is greater than that of TAPT-COF. In addition, TAPT-COF and TAB-COF have good iodine retention and recycling properties for iodine vapour, and have good adsorption capacity for iodine in cyclohexane system. This indicates that thiophene-containing COFs can be used for iodine adsorption in the environment with good adaptability. The study shows that the introduction of

thiophene into COFs improves adsorption efficiency in general, and in particular paves the way for the development of stable and effective COF adsorbents to capture iodine from a variety of environments.

Data availability

The data supporting this article have been included as part of the ESI.†

Author contributions

Yiling Ran: data curation, formal analysis, visualization. Yi Wang: conceptualization, investigation, methodology, funding acquisition, resources, writing – original draft, writing – review & editing. Man Yang: data curation, investigation, validation. Jian Li: data curation, investigation. Yan Zhang: conceptualization, investigation, methodology, writing – original draft, writing – review & editing. Zhanguo Li: conceptualization, investigation, methodology, project administration, supervision, writing – original draft, writing – review & editing.

Conflicts of interest

There are no conflicts of interest to declare.

Acknowledgements

We acknowledge support by the New Iodine Adsorbent Material Project (Grant JCKY2022130C022).

References

1 M. D. Mathew, Nuclear energy: A pathway towards mitigation of global warming, *Prog. Nucl. Energy*, 2022, **143**, 104080.
2 J. Vujic, D. P. Antic and Z. J. E. Vukmirovic, Environmental impact and cost analysis of coal versus nuclear power: The U.S. case, *Energy*, 2012, **45**(1), 31.
3 N. Mokhtari, M. J. S. Dinari and P. Technology, Developing novel amine-linked covalent organic frameworks towards reversible iodine capture, *Sep. Purif. Technol.*, 2022, **301**, 121948.
4 Y. Wang, J. Wang and L. Hou, Reverse osmosis membrane with crown ethers decoration for enhanced radionuclides sieving, *Surf. Interfaces*, 2024, **48**, 1042222.
5 B. J. Riley, J. D. Vienna, D. M. Strachan, J. S. Mccloy and J. Jerden, Materials and processes for the effective capture and immobilization of radioiodine: A review, *J. Nucl. Mater.*, 2016, **470**, 307.
6 R. Liu, W. Zhang, Y. Chen, C. Xu, G. Hu and Z. Han, Highly efficient adsorption of iodine under ultrahigh pressure from aqueous solution, *Sep. Purif. Technol.*, 2020, **233**, 115999.
7 Y. Li, X. Li, J. Li, W. Liu, G. Cheng and H. Ke, Phosphine-based covalent organic framework for highly efficient iodine capture, *Microporous Mesoporous Mater.*, 2021, **325**, 111351.
8 X. Long, C. Ya-Shuo, Q. Zheng, X. Xing-Xiao, H. Tang, J. Li-Ping, J. Juan-Tao and Q. Jian-Hua, Removal of iodine from aqueous solution by PVDF/ZIF-8 nanocomposite membranes, *Sep. Purif. Technol.*, 2020, **238**, 116488.
9 Y. Y. Chen, S. H. Yu, Q. Z. Yao, S. Q. Fu and G. T. Zhou, One-step synthesis of Ag2O@Mg(OH)2 nanocomposite as an efficient scavenger for iodine and uranium, *J. Colloid Interface Sci.*, 2018, **510**, 280.
10 T. Hasell, M. Schmidtmann and A. I. Cooper, Molecular doping of porous organic cages, *J. Am. Chem. Soc.*, 2011, **133**(38), 14920.
11 F. S. Dorina, M. A. Rodriguez and K. W. Chapman, Capture of Volatile Iodine, a Gaseous Fission Product, by Zeolitic Imidazolate Framework-8, *J. Am. Chem. Soc.*, 2011, **133**(32), 12398.
12 M. H. Zeng, Z. Yin, Y. X. Tan, W. X. Zhang, Y. P. He and M. Kurmoo, Nanoporous Cobalt(II) MOF Exhibiting Four Magnetic Ground States and Changes in Gas Sorption upon Post-Synthetic Modification, *J. Am. Chem. Soc.*, 2014, **136**(12), 4680.
13 W. Xie, D. Cui, S. R. Zhang, Y. H. Xu and D. L. Jiang, Iodine capture in porous organic polymers and metal–organic frameworks materials, *Mater. Horiz.*, 2019, **6**, 1571–1595.
14 J. F. Kurisingal, H. Yun and C. S. Hong, Porous organic materials for iodine adsorption, *J. Hazard. Mater.*, 2023, **458**, 131835.
15 J. Huve, A. A. Ryzhikov and A. H. Nouali, Lalia. Porous sorbents for the capture of radioactive iodine compounds: a review, *RSC Adv.*, 2018, **8**, 29248–29273.
16 S. A. Patil, R. R. Rodríguez-Berríos, D. Chavez-Flores, D. V. Wagle and A. Bugarin, Recent Advances in the Removal of Radioactive Iodine and Iodide from the Environment, *ACS ES&T Water*, 2023, **3**(8), 2009.
17 D. Chen, Y. Fu, W. Yu, G. Yu and C. Pan, Versatile Adamantane-based Porous Polymers with Enhanced Microporosity for Efficient CO 2 Capture and Iodine Removal, *Chem. Eng. J.*, 2018, **334**, 900–906.
18 K. Coldsnow, V. Utgikar, P. Sabharwall and D. E. Aston, Capture of harmful radioactive contaminants from off-gas stream using porous solid sorbents for clean environment – A review, *Chem. Eng. J.*, 2016, **306**, 369–381.
19 M. Liu, Q. Xu and G. Zeng, Ionic Covalent Organic Frameworks in Adsorption and Catalysis, *Angew. Chem., Int. Ed.*, 2024, **63**, e202404886.
20 H. Li, D. Zhang, K. Cheng, Z. Li and P.-Z. Li, Effective iodine adsorption by nitrogen-rich nanoporous covalent organic frameworks, *ACS Appl. Nano Mater.*, 2023, **6**(2), 1295.
21 K. Cheng, H. Li, Z. Li, P.-Z. Li and Y. Zhao, Linking nitrogen-rich organic cages into isoreticular covalent organic frameworks for enhancing iodine adsorption capability, *ACS Mater. Lett.*, 2023, **5**(6), 1546.
22 Y. Xie, T. T. Pan and Q. Lei, Ionic Functionalization of Multivariate Covalent Organic Frameworks to Achieve Exceptionally High Iodine Capture Capacity, *Angew. Chem., Int. Ed.*, 2021, **60**, 22432–22440.
23 L. He, L. Chen, X. Dong, S. Zhang, M. Zhang, X. Dai, X. Liu, P. Lin, K. Li and C. Chen, A nitrogen-rich covalent organic

framework for simultaneous dynamic capture of iodine and methyl iodide, *Chem*, 2021, **7**, 699–714.

24 C. Qin, X. Wu, L. Tang, X. Chen, M. Li, Y. Mou, B. Su, S. Wang, C. Feng and J. Liu, Dual donor-acceptor covalent organic frameworks for hydrogen peroxide photosynthesis, *Nat. Commun.*, 2023, **14**(1), 5238.

25 W. Hongtao, N. Jing, C. Xingdi and L. Xuehui, Long.Benzotrithiophene-Based Covalent Organic Frameworks: Construction and Structure Transformation under Ionothermal Condition, *J. Am. Chem. Soc.*, 2018, **140**, 11618–11622.

26 X. Pan, X. Qin, Q. Zhang, Y. Ge and G. J. Cheng, N- and S-rich covalent organic framework for highly efficient removal of indigo carmine and reversible iodine capture, *Microporous Mesoporous Mater.*, 2021, **325**, 111351.

27 C. L. Chen and Y. Li, Synthesis of nitrogen-containing covalent organic framework with reversible iodine capture capability, *Microporous Mesoporous Mater.*, 2021, **312**(1), 110739.

28 S. Song, Y. Shi, N. Liu and F. Liu, C=N linked covalent organic framework for the efficient adsorption of iodine in vapor and solution, *RSC Adv.*, 2021, **11**(18), 10512.

29 X. Yinghui, R. Qiuyu, M. Fengyi, W. Shiyu, W. You, L. Xiaolu, H. Mengjie, C. Zhongshan, Y. Hui, G. I. N. Waterhouse, *et al.*, Engineering the pore environment of antiparallel stacked covalent organic frameworks for capture of iodine pollutants, *Nat. Commun.*, 2024, **15**(1), 2671.

30 Yao, H. Hu, B. Sun, N. Wang, W. Hu and S. Komarneni, Self-Supportive Mesoporous Ni/Co/Fe Phosphosulfide Nanorods Derived from Novel Hydrothermal Electrodeposition as a Highly Efficient Electrocatalyst for Overall Water Splitting, *Small*, 2019, **15**(50), 1905201.

31 J. Fu, J.-Y. Liu, Y.-R. Zhou, L. Zhang, S.-L. Wang, S. Qin, M. Fan, G.-H. Tao and L. He, A novel ionic-liquid-mediated covalent organic framework as a strong electrophile for high-performance iodine removal, *Chem. Eng. J.*, 2024, **488**, 150913.

32 M. Peng, H. Sun, T. Chen, W. Zhang, Z. Zhu, W. Liang and A. Li, A Sponge-Like 3D-PPy Monolithic Material for Reversible Adsorption of Radioactive Iodine, *Macromol. Mater. Eng.*, 2017, **302**, 1700156.

33 X. Yan, Y. Yang, G. Li, J. Zhang, Y. He, R. Wang, Z. Lin and Z. Cai, Thiophene-based covalent organic frameworks for highly efficient iodine capture, *Chin. Chem. Lett.*, 2023, **34**, 107201.

34 W.-Z. She, Q.-L. Wen, H.-C. Zhang, J.-Z. Liu, R. S. Li, J. Ling and Q. Cao, Nanoporous N-rich covalent organic frameworks with high specific surface area for efficient adsorption of iodine and methyl iodide, *ACS Appl. Nano Mater.*, 2023, **6**(19), 18177.

35 B. Ma, Y. Zhou, W. Hu and Y. Zhang, Synthesis and iodine-trapping properties of novel nitrogen-rich imide covalent organic framework materials, *New J. Chem.*, 2024, **48**(4), 1724.

36 N. Farooq, A. Taha and A. Hashmi, Facile synthesis of a nitrogen-rich covalent organic framework for the efficient capture of iodine, *J. Mater. Chem. A*, 2024, **12**(17), 10539.

37 C. Gao and X. Guan, Enhancing the Iodine Adsorption Capacity of Pyrene-Based Covalent Organic Frameworks by Regulating the Pore Environment, *Macromol. Rapid Commun.*, 2023, **44**(19), 2300311.

38 C. Liu, Y. Jin, Z. Yu, L. Gong, H. Wang, B. Yu, W. Zhang and J. Jiang, Transformation of Porous Organic Cages and Covalent Organic Frameworks with Efficient Iodine Vapor Capture Performance, *J. Am. Chem. Soc.*, 2022, **144**(27), 12390.

39 T. Kaiho, Physical Properties of Iodine, *Iodine Chem. Appl.*, 2014, 7, DOI: **10.1002/9781118909911.ch2**.

40 S. Saurabh, S. Mollick, Y. D. More, A. Banerjee, S. Fajal, N. Kumar, M. M. Shirolkar, S. B. Ogale and S. K. Ghosh, Covalent Organic Framework Featuring High Iodine Uptake for Li-Ion Battery: Unlocking the Potential of Hazardous Waste, *ACS Mater. Lett.*, 2023, **5**(9), 2422.